Electronic structure of $Zn_{1-x}Mn_xTe$

M. Taniguchi
Department of Materials Science, Faculty of Science, Hiroshima University, Kagamiyama 1-3, Higashi-Hiroshima 724, Japan

K. Soda
Department of Mathematical Science, College of Engineering, University of Osaka Prefecture, Mozu-Ume-machi, Sakai 591, Japan

I. Souma and Y. Oka
Research Institute for Scientific Measurements, Tohoku University, Katahira, Sendai 980, Japan
(Received 19 April 1991; revised manuscript received 23 March 1992)

The electronic structures of ZnTe and $Zn_{0.7}Mn_{0.3}Te$ have been investigated by means of synchrotron-radiation photoemission experiments. Te 4*d* core-yield spectra of ZnTe and $Zn_{0.7}Mn_{0.3}Te$ reflect the density of states (DOS) of the conduction bands. The two DOS peaks in the ZnTe spectrum observed at 0.6 and 4.3 eV above the conduction-band minimum are ascribed to relatively flat regions of the conduction bands near the L_1 and X_1, and the Γ_{15} and L_3, symmetry points, respectively. The contribution of the Mn 3*d* states to the valence bands of $Zn_{0.7}Mn_{0.3}Te$ has been evaluated by means of resonant enhancement of Mn 3*d* photoionization cross section near the Mn 3*p*-3*d* core excitation. The Mn 3*d*-derived partial DOS of $Zn_{0.7}Mn_{0.3}Te$ is found to be very similar to that of $Cd_{0.8}Mn_{0.2}Te$. This suggests nearly equal Mn-Te bond lengths in these ternary alloys.

INTRODUCTION

$Zn_{1-x}Mn_xTe$ mixed crystals are diluted magnetic semiconductors (DMS's) in which Mn atoms replace Zn atoms in zinc-blende-structure ZnTe for Mn concentrations (x) up to $x=0.86$.[1,2] Such a system has been the subject of intensive investigations because of the interesting magnetic[3,4] and optical properties of DMS's.[5–7] These effects stem from a hybridization of the Mn 3*d* states in the high-spin configuration with the *sp*-band states of the crystal. Therefore, theoretical investigations on Mn-based DMS's (Refs. 8–11) have been focused on the Mn 3*d* contribution to the energy-band structure and on the hybridization between the Mn 3*d*– and anion-derived *p* states. Very recently, the spin-polarized configuration $(3d\uparrow)^5(4s\uparrow)(4p\uparrow)$, instead of $(3d\uparrow)^4(4s)^2$, has been proposed for the ground state of Mn in $Cd_{1-x}Mn_xTe$.[12,13] The electronic structures of antiferromagnetic zinc-blende-structure MnTe (Ref. 12) and the anomalous Curie constants of $Cd_{1-x}Mn_xTe$ (Ref. 13) have been successfully interpreted in terms of such a configuration.

In this paper, we report results of a photoemission study of $Zn_{1-x}Mn_xTe$ using synchrotron radiation. Total-yield spectra of $Zn_{1-x}Mn_xTe$ due to the Te 4*d* core absorption reflect the density of states (DOS) of the conduction bands. Two DOS peaks are ascribed to particularly flat regions of conduction bands on the basis of a comparison with the band structure calculated with use of the modified orthogonalized plane-wave method.[14] Resonant photoemission experiments in the Mn 3*p*-3*d* core-excitation region[15–18] demonstrate that the Mn 3*d* partial DOS of $Zn_{0.7}Mn_{0.3}Te$ is very similar to that of $Cd_{0.8}Mn_{0.2}Te$. This close similarity is discussed with the aid of data on the Mn-Te local coordination in $Cd_{1-x}Mn_xTe$.[19,20]

EXPERIMENT

Total-yield and valence-band photoemission measurements were carried out with synchrotron radiation from SOR-RING (an electron storage ring operated at 380 MeV) at the Institute for Solid State Physics of The University of Tokyo. The total-yield mode was employed to obtain core-absorption spectra. In addition, a combination of a modified Rowland-type monochromator and a double-stage cylindrical mirror analyzer was used to measure the angle-integrated photoemission spectra. Binding energy with respect to the valence-band maximum was determined by extrapolating the steep leading edge of the highest valence-band peak to the baseline. Intensities of the total-yield spectra and valence-band spectra for resonant photoemission experiments were normalized to the monochromator output by the use of the photoelectron yield from Au film, with its quantum yield[21] taken into account.

The backgrounds in the valence-band photoemission spectra due to inelastic secondary electrons were, in some cases, removed from the spectra. Then, we assumed[22] that the intensity of secondary electrons $I_s(E)$ at binding energy E is given by

$$I_s(E)=k\int_{E_0}^{E} I(E')dE' , \quad (1)$$

where $I(E')$, E_0, and k represent, respectively, the total emission intensity at binding energy E', the binding energy corresponding to the highest kinetic energy of the emitted electrons, and a constant. The constant k can be determined by applying (1) to the emission intensity at

binding energy E_a where the entire contribution is only from secondary electrons. Then, k satisfies the following relation:

$$k = \frac{I_s(E_a)}{\int_{E_0}^{E_a} I(E')dE'} . \quad (2)$$

The $Zn_{1-x}Mn_xTe$ and $Cd_{1-x}Mn_xTe$ samples used were undoped single crystals grown by a modified Bridgman method for $0 \leq x \leq 0.3$. Surfaces for the photoemission measurements were prepared *in situ* by cleavage under ultrahigh vacuum ($< 3 \times 10^{-10}$ Torr) in the preparation chamber. The working pressure in the analysis chamber was 7×10^{-11} Torr during the measurements. All measurements were performed at room temperature.

RESULTS AND DISCUSSION

Total-yield spectra are well known to be representative of the absorption spectra in the core-excitation region.[23] Figure 1 shows such absorption spectra of ZnTe and $Zn_{0.7}Mn_{0.3}Te$ in the Te 4*d* and the Mn 3*p* core-excitation regions. Structures due to transitions from the Te 4*d* core levels to the conduction bands are observed in the energy range 40–47 eV. The spectrum of the ZnTe sample exhibits broad peaks at 42.0, 43.5, 45.7, and 47.2 eV. In view of the spin-orbit-splitting energy of the Te 4*d* core levels (1.5 eV), these structures may be classified as two spin-orbit pairs: *A*-*A'* at 42.0 and 43.5 eV and *B*-*B'* at 45.7 and 47.2 eV.

The threshold energy of the core absorption, indicated by a vertical arrow in Fig. 1 for ZnTe, has been estimated to be 41.4 eV from the sum of the binding energy of the Te $4d_{5/2}$ core level with respect to the valence-band maximum (39.2 eV) and the energy of the fundamental band gap at the Γ point (2.2 eV).[5] The binding energies of the Te 4*d* core levels (39.2 and 40.7 eV for the $4d_{5/2}$ and $4d_{3/2}$ core levels, respectively) has been determined from the photoemission measurements. Structures *A* and *B* can thus be assigned to transitions from the Te $4d_{5/2}$ core level into the empty states located 0.6 and 4.3 eV above the conduction-band minimum, respectively.

One notices the absence of intense and sharp peak structures due to core-exciton formation near the core-excitation threshold.[24] All structures observed are rather broad peaks. States at the conduction-band minimum are of nearly pure Zn 4*s* character and the core excitations are charge-transfer transitions with small oscillator strength. This fact may account for the absence of core excitons. Therefore, it is reasonable to assume that the core-excitation spectra map roughly the DOS of the conduction bands. We may then discuss the spectra in terms of the one-electron model, while neglecting the electron–core-hole interaction.

Figure 2 shows the band structure of ZnTe calculated by Kurganskii, Farberovich, and Domashevskaya with use of the modified orthogonalized plane-wave method.[14] The direct fundamental gap is located at the Γ point. The calculated energy gap of 2.6 eV is, however, larger than the experimental value of 2.2 eV. One can recognize flat regions of conduction bands around the L_1, X_1, Γ_{15}, and L_3 symmetry points, which are located 0.8, 1.1, 4.0, and 4.6 eV above the conduction-band minimum (Γ_1), respectively. These flat regions would make a significant contribution to the DOS peaks of the conduction bands. Thus, we attribute structures *A* and *B* to transitions from the Te $4d_{5/2}$ core level to particularly flat regions of the conduction bands near the L_1 and X_1, and the Γ_{15} and L_3 symmetry points, respectively. With x increasing from 0 to 0.3, spectral features of the Te 4*d* core absorption show little change in the form of broadening in the structures.

While the Te 4*d* core-absorption spectra are interpreted in terms of the single-particle band-structure picture, the Mn 3*p* core spectrum of $Zn_{0.7}Mn_{0.3}Te$ in the energy region from 47 to 55 eV exhibits a close resemblance to

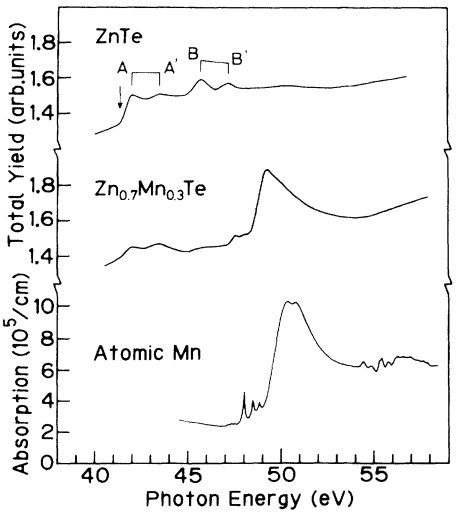

FIG. 1. Total-yield spectra of ZnTe and $Zn_{0.7}Mn_{0.3}Te$ in the Te 4*d* and Mn 3*p* core-excitation regions (Te, 40–47 eV; Mn, 47–58 eV). The absorption threshold of the Te 4*d* core spectrum is indicated by a vertical arrow. The absorption spectrum due to the Mn 3*p*-3*d* core excitations in atomic Mn (Ref. 25) is also shown for comparison.

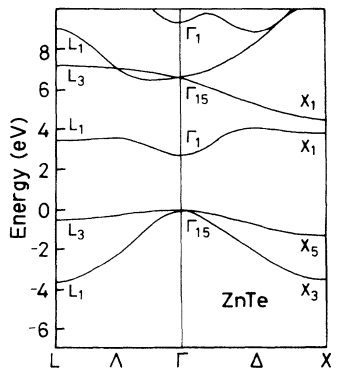

FIG. 2. ZnTe energy bands calculated by Kurganskii, Farberovich, and Domashevskaya using the modified orthogonalized plane-wave method (Ref. 14). The energy origin is referred to the valence-band maximum.

that of atomic Mn,[25] which is also shown in Fig. 1, for comparison. The prominent absorption band at 50 eV in the spectrum of the atomic Mn is due to a transition from the $3p^63d^54s^2(^6S)$ ground state of the Mn atom into the $3p^53d^64s^2(^6P)$ excited state.[26,27] Three small peaks at lower energies correspond to transitions into the ^6D and ^4P members of the $3p^53d^6$ multiplet, respectively. The ^6P transition is strongly enhanced by a Fano resonance with the degenerate continuum transition from the $3p^63d^54s^2$ ground state into the $3p^63d^44s^2\varepsilon f$ state, which is also responsible for its width and the asymmetric line shape.

Next, we consider the valence bands. Figure 3 exhibits the valence-band photoemission spectra of ZnTe and $Zn_{0.7}Mn_{0.3}Te$ measured at an excitation photon energy ($\hbar\omega$) of 60 eV. The valence-band spectrum of pure ZnTe has been previously reported by several authors and discussed in detail.[28,29] We recall here that the two prominent peaks at 1.7 and 4.8 eV binding energies reflect the maxima in the DOS of the valence bands, which are primarily derived from Te 5p states (p valence bands) with an increasing contribution from the Zn 4s states toward deeper binding energy. The L_3, X_5, $\Sigma_1^{\min}$, and L_1 symmetry points indicated for the spectrum of ZnTe are the ones contributing to the DOS structures.[28] With x increasing from 0 to 0.3, another Mn-derived emission peak appears between the two prominent p-valence-band peaks at 1.7 and 4.8 eV binding energies, though there is no discernible change in the shape of the sp valence bands except for a slight blurring of the fine structures.

The identification of the Mn-derived states is further facilitated by the use of tunable synchrotron radiation. One can evaluate a measure of the Mn 3d-derived partial DOS and investigate the degree of hybridization from resonant photoemission experiments.[15–17] The resonance takes place over a specific energy range as a result of the interference between the direct excitation process of the Mn 3d electrons ($3p^63d^5+\hbar\omega\rightarrow 3p^63d^4+\varepsilon f$) and the discrete Mn 3$p-3d$ core-excitation process followed by a super-Coster-Kronig decay ($3p^63d^5+\hbar\omega \rightarrow 3p^53d^6, 3p^53d^6\rightarrow 3p^63d^4+\varepsilon f$). Since only the Mn 3$d$ states are resonantly enhanced for $\hbar\omega$ near the Mn 3p-3d core excitation, one can estimate quantitatively their contribution to the valence-band DOS by comparing the spectra taken just on and off resonance.[15,16] The cross sections of other valence-band states, such as the Te 5p, Zn 4s, and 4p states, do not vary appreciably over a small energy range around the resonance.

Figure 4 shows a series of $Zn_{0.7}Mn_{0.3}Te$ valence-band spectra for $\hbar\omega$ near the Mn 3p-3d core excitation. In the figure, spectral intensities have been normalized to the monochromator output; thus the spectra can be compared not only with respect to their shape but also in terms of relative intensities. One notices a prominent resonance for the peak at 3.75 eV binding energy. The intensity of this peak reaches its maximum at $\hbar\omega=49.5$ eV. The remainder of the valence bands is also resonantly enhanced. In particular, a set of states appears between 6 and 8 eV binding energy near the resonance. In Fig. 4, we cannot clearly recognize the expected Mn $M_{2,3}M_{4,5}M_{4,5}$ Auger peak, which moves through the spectra upon increasing photon energies above the resonance.[30] This suggests that the prominent decay channel of the Mn 3p-3d core excitation may be direct recombination rather than Auger decay, consistent with the fairly localized nature of the excitation. Similar phenomenon has also been reported in $Cd_{1-x}Mn_xTe$.[15]

In order to investigate the resonant profile in detail, we plot the photoemission intensities of selected valence-band features as a function of $\hbar\omega$ in Fig. 5, where each

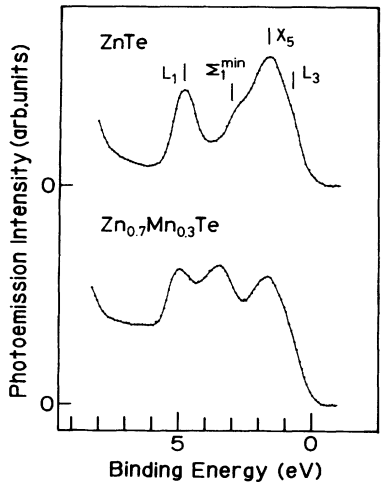

FIG. 3. Valence-band photoemission spectra of ZnTe and $Zn_{0.7}Mn_{0.3}Te$ measured at $\hbar\omega=60$ eV. The symmetry points contributing to the DOS peaks of ZnTe are shown. The spectrum of $Zn_{0.7}Mn_{0.3}Te$ exhibits a Mn-derived peak between the two prominent p-valence-band peaks of ZnTe. The binding energy is given relative to the valence-band maximum.

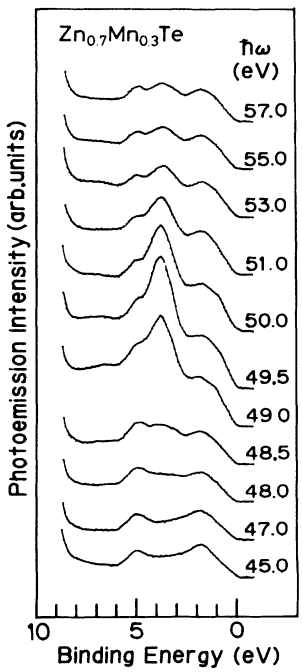

FIG. 4. A series of valence-band spectra of $Zn_{0.7}Mn_{0.3}Te$ for $\hbar\omega$ near the Mn 3p-3d core excitation. The peak at 3.75 eV indicates a prominent resonance.

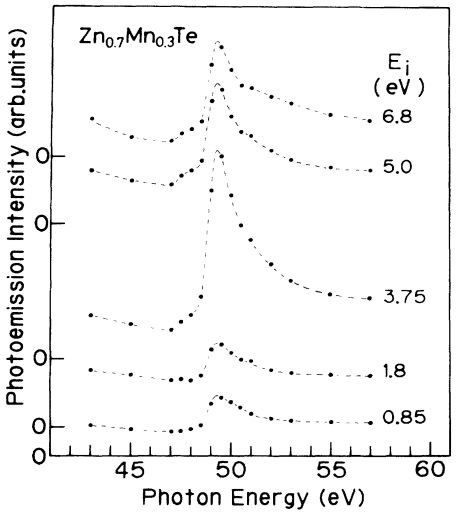

FIG. 5. Photoemission intensities of selected valence bands as a function of $\hbar\omega$. Each valence band is labeled by the binding energy (E_i) with respect to the valence-band maximum.

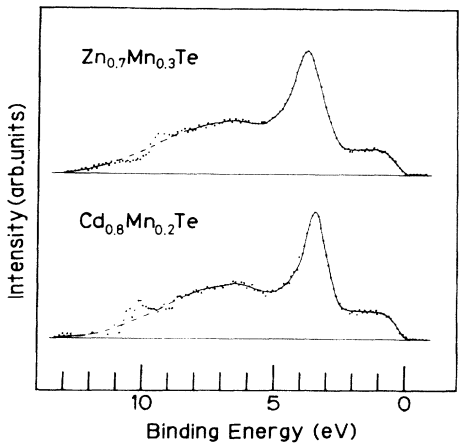

FIG. 6. Mn $3d$-derived partial DOS of $Zn_{0.7}Mn_{0.3}Te$ (upper curve) obtained from the valence-band photoemission spectra measured at the antiresonance ($\hbar\omega=47.0$ eV) and on resonance ($\hbar\omega=49.5$ eV). The $Cd_{0.8}Mn_{0.2}Te$ partial DOS (lower curve) is also shown for comparison. The contribution due to inelastic secondary electrons has been removed.

valence band is specified by the binding energy (E_i) with respect to the valence-band maximum. One notices again that the spectrum for $E_i=3.75$ eV shows a prominent Fano-type resonance. With increasing $\hbar\omega$, the intensity of this structure first decreases gradually to a minimum at 47 eV, and then increases sharply to reach a maximum at 49.5 eV. The spectra for $E_i=0.85$ and 1.8 eV also exhibit a remarkable resonance. The amount of enhancement is as much as about one-quarter of that for the spectrum for $E_i=3.75$ eV. The $E_i=5.0$ and 6.8 eV spectra have contributions in the background due to inelastic secondary electrons. After the correction of this background contribution,[22] however, we obtain still a sizable resonance. The correlation of the valence-band resonance with the Mn $3p$-$3d$ core excitation is clear from a comparison with the corresponding absorption spectra of $Zn_{0.7}Mn_{0.3}Te$ and atomic Mn in Fig. 1.

Here, we deduce a measure of the Mn $3d$ contribution to the valence-band DOS of $Zn_{0.7}Mn_{0.3}Te$ by subtracting the spectrum measured at the antiresonance (47.0 eV) from that taken just on resonance (49.5 eV), after the normalization of spectral intensities to the monochromator output.[15] The result is shown in the upper panel of Fig. 6,[31] where the contribution due to inelastic secondary electrons has been removed by use of the above-mentioned procedure.[22] We find a main peak at 3.75 eV below the valence-band maximum and an appreciable Mn $3d$ contribution throughout the valence-band region from 0 to 5 eV binding energy. In addition, the difference spectrum shows satellite structure at 5–9 eV binding energy.

Previously, we have analyzed the Mn $3d$ partial DOS of $Cd_{1-x}Mn_xTe$ in terms of a cluster model on the basis of a configuration-interaction calculation.[15,16] The photoemission between 0 and 5 eV binding energy has been assigned to $d^5\underline{L}$ final states, which represents final states with a photoproduced d hole screened by charge transfer from the Te $5p$-derived bands. Here, the $\underline{L}$ denotes a ligand hole. Features between 5 and 9 eV binding energy, on the contrary, are ascribed to a satellite with d^4 final states without significant $L\rightarrow d$ screening.

In Fig. 6, we compare the Mn $3d$ partial DOS of $Zn_{0.7}Mn_{0.3}Te$ with that of $Cd_{0.8}Mn_{0.2}Te$.[32] One notices little difference between these DOS spectra except for the energy positions of the sharp peaks (3.75 eV for $Zn_{0.7}Mn_{0.3}Te$ and 3.4 eV for $Cd_{0.8}Mn_{0.2}Te$, respectively). The spectrum of $Cd_{1-x}Mn_xTe$ has been reproduced using parameters such as $\varepsilon_d-\varepsilon_p+U=3.5$ eV and $(pd\pi)=0.47$ eV,[15] where ε_d and ε_p are the energies of unhybridized Mn $3d\uparrow$ and Te $5p$ orbitals ($\uparrow$ and $\downarrow$) and U (7.5 eV) is the Coulomb correlation energy of Mn $3d$ electrons.[33] $(pd\pi)$ exhibits the p-d transfer integral and the ratio $(pd\sigma)/(pd\pi)$ is fixed at -2.16 according to the results of transition-metal pseudopotential theory.[34]

In the configuration-interaction model, the spectral shape of the Mn $3d$ partial DOS depends on values of $\varepsilon_d-\varepsilon_p+U$ and the p-d transfer integrals.[16] For higher values of the p-d transfer integrals or for larger $\varepsilon_d-\varepsilon_p+U$, the valence-band intensity from 0 to 2 eV binding energy relative to the main peak at 3.4 eV binding energy increases, while the satellite intensity between 5 and 9 eV binding energy decreases. The energies ε_p, ε_d, and U do not noticeably change between $Zn_{1-x}Mn_xTe$ and $Cd_{1-x}Mn_xTe$. On the other hand, the p-d transfer-integral values, which depend on the Mn-Te bond length (d), are proportional to $d^{-3.5}$ (Ref. 34).

The bond lengths of pure ZnTe and CdTe are 2.64 and 2.80 Å, respectively. Here, we assume tentatively that the Mn-Te bond length in $Zn_{1-x}Mn_xTe$ was 94% of that in $Cd_{1-x}Mn_xTe$. Then, we obtain the $(pd\pi)$ value of 0.58 eV for $Zn_{1-x}Mn_xTe$ as compared with 0.47 eV for $Cd_{1-x}Mn_xTe$. Change of the $(pd\pi)$ value from 0.47 to 0.58 eV brings a significant modification to the shape of the Mn $3d$ partial DOS.[16] The valence-band intensity

relative to the main peak increases by ~33% and the satellite intensity decreases by ~23%, in contrast to the present results. The close similarity of the Mn 3*d* partial DOS in Fig. 6, thus, suggests almost equal $Zn_{1-x}Mn_xTe$ and $Cd_{1-x}Mn_xTe$ Mn-Te bond lengths, or $(pd\pi)$ values.

EXAFS experiments on $Cd_{1-x}Mn_xTe$ recently performed by Balzarotti *et al.*[19] have revealed that the Cd-Te and Mn-Te bond lengths remain almost unchanged for $0 \leq x \leq 0.4$. The Cd-Te bond length is approximately constant with its value of pure CdTe. In addition, the Mn-Te bond length is approximately equal to that predicted for the hypothetical zinc-blende-structure MnTe. A model of the microscopic structure for $Cd_{1-x}Mn_xTe$ based on a random distribution of cations has been also proposed[20] in excellent agreement with observation. The model describes the bimodal distribution of near-neighbor distances in terms of a distortion of the anion sublattice, where the cation sublattice is assumed to remain fixed.

These ideas[20] are expected to apply to other random ternary zinc-blende-structure alloys, such as $Zn_{1-x}Mn_xTe$. Namely, the Mn-Te bond length in $Zn_{1-x}Mn_xTe$ would be almost equal to that predicted for the hypothetical zinc-blende-structure MnTe. Thus, the *p-d* transfer integrals are assumed to be almost equal to each other between $Zn_{1-x}Mn_xTe$ and $Cd_{1-x}Mn_xTe$. We believe that this is the reason why the spectral shape of the Mn 3*d* partial DOS of $Zn_{1-x}Mn_xTe$ is very similar to that of $Cd_{1-x}Mn_xTe$.

In spite of the many-body nature of the $d^5\underline{L}$ final states, we find a rather good correspondence between the spectral density from 0 to 5 eV binding energy and the one-electron valence-band DOS.[9] Mn 3*d*–Te 5*p* hybridization allows for sufficient screening of the 3*d* excitations by $L \rightarrow d$ charge transfer in the valence bands. In this sense, the spectral density from 0 to 5 eV binding energy in the partial DOS of $Zn_{1-x}Mn_xTe$ and $Cd_{1-x}Mn_xTe$ may be assumed to be a good approximation of a measure of the valence-band DOS. A sharp peak observed at 3.75 eV for $Zn_{1-x}Mn_xTe$ is assigned to emission from Mn $3d\uparrow$ states with e_g symmetry, while the t_{2g} components ($\uparrow$ and $\downarrow$) hybridize appreciably with the Te 5*p* states ($\uparrow$ and $\downarrow$) and spread over the top 5-eV valence bands.[15,16] The close similarity of the Mn 3*d* partial DOS features between $Zn_{1-x}Mn_xTe$ and $Cd_{1-x}Mn_xTe$ may also be understood qualitatively on the basis of a single-particle band-structure picture, assuming that the Mn-Te bond lengths in the two ternary alloys are close to each other.

Recent work on $Zn_{1-x}Mn_xC^{VI}$ (C^{VI}=S, Se, Te) by Weidemann *et al.*[35,36] has come to our attention. The constant-initial-state (CIS) spectra of $Zn_{0.68}Mn_{0.32}Te$ in Ref. 35 exhibit a weak trend of Fano's asymmetry parameter q from 2.4 to 1.8, when the initial-state energy (E_i) is changed from 5.5 to 1.5 eV. Such a trend is approximately consistent with that in the present study in sign and magnitude of the parameters. The spectrum for $E_i = 3.75$ eV in Fig. 5 is reproduced fairly well using parameters of $q = 2.4$ and the full width at half maximum (Γ) of 1.5 eV allowing for an instrumental broadening of 0.18 eV, while the corresponding CIS spectrum in Ref. 35 has been described by fitting parameters of $q = 2.2$ and $\Gamma = 1.9$ eV. A similar trend has been also reported on $Cd_{1-x}Mn_xTe$.[15]

The branching ratios (BR's) of the satellite intensity relative to the main peak in the Mn 3*d* partial DOS features of $Zn_{1-x}Mn_xC^{VI}$ (C^{VI}=S, Se, Te) decrease on going from S to Te, while for valence bands a minimum BR value is found for $Zn_{0.81}Mn_{0.19}Se$,[35] in contrast to the case of $Cd_{1-x}Mn_xC^{VI}$ (C^{VI}=S, Se, Te).[15] Assuming nearly equal Mn-C^{VI} bond lengths for $Zn_{1-x}Mn_xC^{VI}$ and $Cd_{1-x}Mn_xC^{VI}$, however, the Mn 3*d* partial DOS features for alloys with the same anion should be very similar to each other.

The exchange splitting energy of an almost intraionic property of the Mn^{2+} ion estimated for $Zn_{1-x}Mn_xTe$ (5.1 eV) (Ref. 35) seems to be at variance with the Coulomb correlation energy proposed previously for $Cd_{1-x}Mn_xTe$ (7.5 eV).[16] There is no inconsistency, however, since the value reported for $Zn_{1-x}Mn_xTe$ is only a measure of the lower limit of the exchange energy.

Finally, Weidemann *et al.* point out the possibility of an x dependence in the valence-band intensity in the partial DOS features of $Zn_{1-x}Mn_xC^{VI}$ (C^{VI}=S, Se, Te).[35] They quote a recent study on surface and bulk $Cd_{1-x}Mn_xTe$ alloys, which reports the x dependence of the satellite intensity.[37] We find, however, no remarkable difference in the Mn 3*d* partial DOS features of bulk $Cd_{1-x}Mn_xTe$ alloys for $x = 0.2$ and 0.65.[38] To resolve this controversy, further theoretical and experimental studies will be required.

ACKNOWLEDGMENTS

The authors are grateful to Professor A. Fujimori of The University of Tokyo for illuminating discussions on configuration-interaction calculations. We thank Dr. T. Yokoyama of Hiroshima University for valuable discussion on EXAFS. We also thank the staff of SRL-ISSP for the operation of SOR-RING and for their technical support.

[1] A. Pajaczkowska, Prog. Cryst. Growth Charact. **1**, 289 (1978).

[2] *Dilute Magnetic Semiconductors,* Vol. 25 of Semiconductors and Semimetals, edited by J. K. Furdyna and J. Kossut (Academic, New York, 1988).

[3] D. Diouri, J. P. Lascary, and M. El Amrani, Phys. Rev. B **31**, 7995 (1985).

[4] D. L. Peterson, D. U. Bartholomew, U. Debska, A. K. Ramdas, and S. Rodriguez, Phys. Rev. B **32**, 323 (1985).

[5] R. Brun de Re, T. Donofro, J. Avon, J. Magid, and J. C. Wooley, Nuovo Cimento **2D**, 1911 (1983).

[6] G. Barilero, C. Rigaux, M. Menant, Nguyen Hy Hau, and W. Giriat, Phys. Rev. B **32**, 5144 (1985).

[7]S. Ves, K. Strössner, W. Gebhaldt, and M. Cardona, Phys. Rev. B **33**, 4077 (1986).
[8]B. E. Larson, K. C. Hass, H. Ehrenreich, and A. E. Carlsson, Solid State Commun. **56**, 347 (1985).
[9]H. Ehrenreich, K. C. Hass, N. F. Johnson, B. E. Larson, and R. J. Lampert, in *Proceedings of the 18th International Conference on the Physics of Semiconductors, Stockholm, 1986,* edited by O. Engström (World Scientific, Singapore, 1987), pp. 1751–1754.
[10]S.-H. Wei and A. Zunger, Phys. Rev. B **35**, 2340 (1987); Phys. Rev. Lett. **56**, 2391 (1986).
[11]M. Podgórny, Z. Phys. B **69**, 501 (1988).
[12]A. Franciosi, A. Wall, Y. Gao, J. H. Weaver, M.-H. Tsai, J. D. Dow, R. V. Kasowski, R. Reifenberger, and F. Pool, Phys. Rev. B **40**, 12 009 (1989).
[13]M.-H. Tsai, J. D. Dow, R. V. Kasowski, A. Wall, and A. Franciosi, Solid State Commun. **69**, 1131 (1989).
[14]S. I. Kurganskii, O. V. Farberovich, and E. P. Domashevskaya, Fiz. Tekh. Poluprovodn. **14**, 1315 (1980) [Sov. Phys. Semicond. **14**, 775 (1980)].
[15]L. Ley, M. Taniguchi, J. Ghijsen, R. L. Johnson, and A. Fujimori, Phys. Rev. B **35**, 2839 (1987).
[16]M. Taniguchi, A. Fujimori, M. Fujisawa, T. Mori, I. Souma, and Y. Oka, Solid State Commun. **62**, 431 (1987).
[17]M. Taniguchi, A. Fujimori, and S. Suga, Solid State Commun. **70**, 191 (1989).
[18]A. Wall, A. Franciosi, D. W. Niles, R. Reifenberger, C. Quaresima, M. Capozi, and P. Perfetti, Phys. Rev. B **41**, 5969 (1990).
[19]A. Balzarotti, M. Czyżyk, A. Kisiel, N. Motta, M. Podgórny, and M. Zimnal-Starnawska, Phys. Rev. B **30**, 2295 (1984).
[20]A. Balzarotti, N. Motta, A. Kisiel, M. Zimnal-Starnawska, M. T. Czyżyk, and M. Podgórny, Phys. Rev. B **31**, 7526 (1985).
[21]H. J. Hagenmann, W. Gudat, and C. Kunz, J. Opt. Soc. Am. **65**, 742 (1975).
[22]D. A. Shirley, Phys. Rev. B **5**, 4709 (1972); K. Soda, T. Mori, M. Taniguchi, S. Asaoka, K. Naito, Y. Onuki, T. Komatsubara, S. Sato, and T. Ishii, J. Phys. Soc. Jpn. **55**, 1709 (1986). Experimental data in the binding-energy region between 14 and -1 eV have been used for the background subtraction.
[23]W. Gudat and C. Kunz, Phys. Rev. Lett. **29**, 169 (1972).
[24]M. Taniguchi, R. L. Johnson, J. Ghijsen, and M. Cardona, Phys. Rev. B **42**, 3634 (1990).
[25]R. Bruhn, B. Sonntag, and H. W. Wolff, Phys. Lett. **69A**, 9 (1978).
[26]L. C. Davis and L. A. Feldkamp, Phys. Rev. A **17**, 2012 (1978).
[27]S. Nakai, H. Nakamori, A. Tomita, K. Tsutsumi, H. Nakamura, and C. Sugiura, Phys. Rev. B **9**, 1870 (1974).
[28]L. Ley, A. Pollak, F. R. McFeely, S. P. Kowalczyk, and D. A. Shirley, Phys. Rev. B **9**, 600 (1974), and references therein.
[29]N. J. Shevchik, J. Tejeda, and M. Cardona, Phys. Rev. B **9**, 2627 (1974), and references therein.
[30]We found a broad emission band around 16 eV binding energy in the spectrum taken at $\hbar\omega=57$ eV for $Zn_{0.4}Mn_{0.6}Te$ instead of the $Zn_{0.7}Mn_{0.3}Te$ sample in Fig. 4. The energy of the structure moves from 16 toward 13 eV changing $\hbar\omega$ from 57 to 54 eV. The emission intensity of the structure at 16 eV (or 13 eV) binding energy is, however, very weak and is estimated to be, at most, $\sim 10\%$ of that of the valence-band peak at 1.7 eV binding energy, after background subtraction. We suppose that the intensity of the expected Mn $M_{2,3}M_{4,5}M_{4,5}$ Auger emission would be fairly weak in the spectrum for $Zn_{0.7}Mn_{0.3}Te$ with a smaller x than $Zn_{0.4}Mn_{0.6}Te$. For $Cd_{1-x}Mn_xTe$, a discussion on the Mn $M_{2,3}M_{4,5}M_{4,5}$ Auger emission has already been made in detail in Ref. 15 on the basis of experimental data of valence-band and CIS spectra.
[31]The method employed for the evaluation of the Mn 3*d* partial DOS in Fig. 6 does not take into account the variation of the Cd 4*d* and the Te 5*s* emission with $\hbar\omega$, both present in the 9–12-eV binding-energy region, or the modulation in the relative intensity between the Cd 4*d* surface and bulk components, since these quantities would not vary appreciably in the small range of $\hbar\omega$ (47.0–49.5 eV). Such factors, as well as insufficient statistics of experimental data, produce features which do not reflect the Mn 3*d* partial DOS in the 9–12-eV binding-energy region. The Mn 3*d* contributions in this energy region are, thus, extrapolated and drawn by broken lines in Fig. 6.
[32]The Mn 3*d* partial DOS features of $Zn_{0.7}Mn_{0.3}Te$ and $Cd_{0.8}Mn_{0.2}Te$ have been obtained by using the same procedure as that described in the text.
[33]O. Gunnarsson, A. V. Postnikov, and O. K. Andersen, Phys. Rev. B **40**, 10 407 (1989).
[34]W. A. Harrison, *Electronic Structure and the Properties of Solids* (Freeman, San Francisco, 1980).
[35]R. Weidmann, H. E. Gumlich, M. Kupsch, H.-U. Middelmann, and U. Becker, Phys. Rev. B **45**, 1172 (1992).
[36]Valence-band photoemission spectra of Zn C^{VI} (C^{VI}=S, Se, Te) binary alloys in Ref. 35 measured for surface prepared by Ar-ion sputtering and annealing after cleavage in the atmosphere are somewhat different from those previously reported (Refs. 28 and 29) with respect to their spectral shape and additional structure. In addition, the spectral features of $Zn_{1-x}Mn_xTe$ ternary alloys for $x=0$ and 0.32 in Ref. 35 are not exactly in agreement with those for $x=0$ and 0.3 in the present study. The valence-band photoemission spectra of $Zn_{1-x}Mn_xC^{VI}$ (C^{VI}=S, Se, Te) should be compared with those obtained for surfaces prepared *in situ* by cleavage in ultrahigh vacuum.
[37]A. Wall, A. Raisanen, G. Haugstad, L. Vanzetti, and A. Franciosi, Phys. Rev. B **44**, 8185 (1991).
[38]The satellite intensity relative to the main peak of bulk $Cd_{1-x}Mn_xTe$ in Ref. 37 increases from 0.19 to 0.37 with x increasing from 0.2 to 0.6, where intensities of the structures are evaluated with respect to the linear background extrapolated between 0 and 16–17 eV binding energies. We find, on the other hand, that the relative intensities of the satellite are in the range of 0.45 ± 0.03 for bulk $Cd_{1-x}Mn_xTe$ alloys with $x=0.2$ and 0.65, after the background subtraction described in the text.